
Score Normalization for a Faster Diffusion Exponential Integrator Sampler

Guoxuan Xia^{1*} Duolikun Danier^{2*} Ayan Das³ Stathi Fotiadis^{1,3}
Farhang Nabiei³ Ushnish Sengupta³ Alberto Bernacchia³

¹Imperial College London, UK ²University of Bristol, UK ³MediaTek Research, UK
g.xia21@imperial.ac.uk duolikun.danier@bristol.ac.uk
{first.last}@mtkresearch.com

Abstract

Recently, Zhang and Chen [25] have proposed the Diffusion Exponential Integrator Sampler (DEIS) for fast generation of samples from Diffusion Models. It leverages the *semi-linear* nature of the probability flow ordinary differential equation (ODE) in order to greatly reduce integration error and improve generation quality at low numbers of function evaluations (NFEs). Key to this approach is the *score function reparameterisation*, which reduces the integration error incurred from using a fixed score function estimate over each integration step. The original authors use the default parameterisation used by models trained for noise prediction – multiply the score by the standard deviation of the conditional forward noising distribution. We find that although the mean absolute value of this score parameterisation is close to constant for a large portion of the reverse sampling process, it changes rapidly at the end of sampling. As a simple fix, we propose to instead reparameterise the score (at inference) by dividing it by the average absolute value of previous score estimates at that time step collected from offline high NFE generations. We find that our score normalisation (DEIS-SN) consistently improves FID compared to vanilla DEIS, showing an improvement at 10 NFEs from 6.44 to 5.57 on CIFAR-10 and from 5.9 to 4.95 on LSUN-Church (64×64). Our code is available at <https://github.com/mtkresearch/Diffusion-DEIS-SN>.

1 Introduction

Diffusion models [4, 20] have emerged as a powerful class of deep generative models, due to their ability to generate diverse, high-quality samples, rivaling the performance of GANs [8] and autoregressive models [19]. They have shown promising results across a wide variety of domains and applications including (but not limited to) image generation [2, 17], audio synthesis [12], molecular graph generation [6], and 3D shape generation [16]. They work by gradually adding Gaussian noise to data through a forward diffusion process parameterized by a Markov chain, and then reversing this process via a learned reverse diffusion model to produce high-quality samples.

The sampling process in diffusion models can be computationally expensive, as it typically requires hundreds to thousands of neural network function evaluations to generate high-quality results. Moreover, these network evaluations are necessarily *sequential*, seriously hampering generation latency. This has motivated recent research efforts to develop acceleration approaches that allow the generation of samples with fewer function evaluations while maintaining high sample quality. Denoising Diffusion Implicit Models (DDIM) [21] is an early but effective acceleration approach that proposes a non-Markovian noising process for more efficient sampling. Song et al. [22] show that samples can be

*Work done whilst interning at MediaTek Research.



Figure 1: Generations at 5 NFEs with a CIFAR-10 model. Top: DEIS-SN (ours). Bottom: DEIS [25]. It can be seen that DEIS-SN is often able to better generate details (such as wheels on cars). More generation results are shown in Fig. 4 of Appendix D.

quickly generated by using black-box solvers to integrate a probability flow ordinary differential equation (ODE). Differentiable Diffusion Sampler Search (DDSS) [24] treats the design of fast samplers for diffusion models as a differentiable optimization problem. Diffusion model sampling with neural operator (DSNO) [27] accelerates the sampling process of diffusion models by using neural operators to solve probability flow differential equations. Progressive Distillation [18] introduces a method to accelerate the sampling process by iteratively distilling the knowledge of the original diffusion model into a series of models that learn to cover progressively larger and larger time step sizes.

Recently, a new family of fast samplers, that leverage the *semi-linear* nature of the probability flow ODE, have enabled new state-of-the-art results at low numbers of function evaluations (NFEs) [13, 25, 26]. In this work we focus on improving the Diffusion Exponential Integrator Sampler (DEIS) [25], specifically the time-based Adams-Bashforth version (DEIS-*t*AB). Our contributions are as follows:

1. We show that DEIS’s default score parameterisation’s average absolute value varies rapidly near the end of the reverse process, potentially leading to additional integration error.
2. We propose a simple new score parameterisation – to normalise the score estimate using its average empirical absolute value at each timestep (computed from high NFE offline generations). This leads to *consistent improvements in FID compared to vanilla DEIS*.

2 Preliminaries

Forward Process We define a *forward process* over time $t \in [0,1]$ for random variable $\mathbf{x}_t \in \mathbb{R}^D$,

$$p(\mathbf{x}_t|\mathbf{x}_0) = \mathcal{N}(\mathbf{x}_t; a_t\mathbf{x}_0, \sigma_t^2\mathbf{I}) \quad (1)$$

for \mathbf{x}_0 drawn from some unknown distribution $p(\mathbf{x}_0)$. Here, a_t and σ_t define the *noise schedule*.² The following stochastic differential equation has the same conditional distributions as Eq. (1) [9],

$$d\mathbf{x}_t = f_t\mathbf{x}_tdt + g_t d\mathbf{w}_t, \quad \mathbf{x}_0 \sim p(\mathbf{x}_0), \quad (2)$$

where $\mathbf{w}_t \in \mathbb{R}^D$ is the Wiener process and

$$f_t = \frac{da_t}{dt} \frac{1}{a_t}, \quad g_t^2 = \frac{d\sigma_t^2}{dt} - 2f_t\sigma_t^2. \quad (3)$$

Probability Flow ODE Song et al. [22] show that the following ODE,

$$\frac{d\mathbf{x}_t}{dt} = f_t\mathbf{x}_t - \frac{1}{2}g_t^2\nabla_{\mathbf{x}_t}\log p(\mathbf{x}_t), \quad \mathbf{x}_1 \sim p(\mathbf{x}_1), \quad (4)$$

shares the same marginal distributions $p(\mathbf{x}_t)$ as the stochastic differential equation in Eq. (2). Given a neural network that is trained to approximate the score $\mathbf{s}_\theta(\mathbf{x}_t, t) \approx \nabla_{\mathbf{x}_t}\log p(\mathbf{x}_t)$, Eq. (4) can be exploited to generate samples approximately from $p(\mathbf{x}_0)$ using blackbox ODE solvers [22]. This approach tends to produce higher quality samples at lower NFEs vs stochastic samplers [22]. We note that in the domain of diffusion models, neural networks tend to be trained to predict a *parameterisation* of the score, e.g. $\mathbf{s}_\theta(\mathbf{x}_t, t) = -\epsilon_\theta(\mathbf{x}_t, t)/\sigma_t$ (noise prediction) [4] or $\mathbf{s}_\theta(\mathbf{x}_t, t) = (a_t\mathbf{x}_\theta(\mathbf{x}_t, t) - \mathbf{x}_t)/\sigma_t^2$ (sample prediction) [18], as this leads to better optimisation and generation quality [4].

²Note that we restrict ourselves to the case of isotropic noising as it applies to the vast majority of cases, although it is easy to generalise Eq. (1) by replacing a_t, σ_t^2 with matrices $\mathbf{A}_t, \mathbf{\Sigma}_t$.

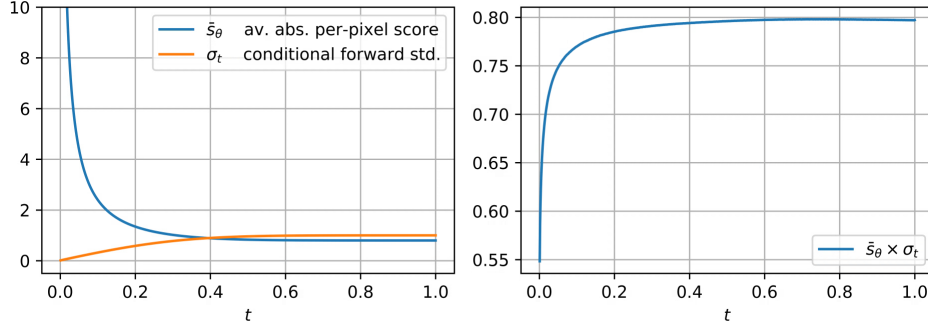


Figure 2: Left: average absolute per-pixel score estimate value \bar{s}_θ and the conditional forward standard deviation σ_t plotted over the reverse process. Right: the product of the previous two values – we see that this is constant for most of the reverse process, but it changes rapidly near $t=0$. The noising schedule is the Linear β schedule [4], the training data is CIFAR-10 and we average 256 samples.

Exponential Integrator Recently, a number of different approaches have exploited the *semi-linear* structure of Eq. (4), solving the linear part, $f_t \mathbf{x}_t$, exactly [13, 14, 25, 26]. This has lead to impressive generation quality at low NFEs (≤ 20). One such approach is the Diffusion Exponential Integrator Sampler (DEIS)³ [25] that uses the following iteration over time grid $\{t_i\}_{i=0}^N$ to generate samples:⁴

$$\mathbf{x}_{t_{i-1}} = \Psi(t_{i-1}, t_i) \mathbf{x}_{t_i} + \sum_{j=0}^r C_{ij} \underbrace{(-K_{t_{i+j}}) \mathbf{s}_\theta(\mathbf{x}_{t_{i+j}}, t_{i+j})}_{\text{score reparameterisation}}, \quad (5)$$

$$C_{ij} = \int_{t_i}^{t_{i-1}} \frac{1}{2} \Psi(t_{i-1}, \tau) g_\tau^2 K_\tau^{-1} \prod_{k \neq j} \left[\frac{\tau - t_{i+k}}{t_{i+j} - t_{i+k}} \right] d\tau,$$

where $\Psi(t, s)$ satisfies $\frac{\partial \Psi(t, s)}{\partial t} = f_t \Psi(t, s)$, $\Psi(s, s) = 1$, K_t is a function used to reparameterise the score estimate and r is the order of the polynomial used to extrapolate said score reparameterisation. We note that C_{ij} and $\Psi(t, s)$ can be straightforwardly calculated offline using numerical methods.

3 The Importance of Score Reparameterisation

The key to reducing integration error in Eq. (5) is the score reparameterisation. DEIS approximates an integral over $\tau \in [t_{i-1}, t_i]$, over which $-K_\tau \mathbf{s}_\theta(\mathbf{x}_\tau, \tau)$ should vary, using fixed estimates from finite t s. *This approximation will be more accurate the less $-K_\tau \mathbf{s}_\theta(\mathbf{x}_\tau, \tau)$ varies with τ .* Zhang and Chen [25] choose the default parameterisation for noise prediction models, $K_t = \sigma_t$, where $\epsilon_\theta(\mathbf{x}_t, t) = -\sigma_t \mathbf{s}_\theta(\mathbf{x}_t, t)$. Fig. 2 shows that this reparameterisation (right) is roughly constant in average absolute pixel value ($\bar{s}_\theta \sigma_t$) for the majority of the generation process,⁵ whilst the score estimate varies considerably more. By reducing the variation over time of the score estimate via reparameterisation, DEIS is able to achieve much lower integration error and better quality generations at low NFEs [25].

4 Score Normalisation (DEIS-SN)

Fig. 2 also shows, however, that near $t=0$ there is still substantial variation in $\bar{s}_\theta \sigma_t$. Thus we propose a new score reparameterisation, where we simply set $K_t = 1/\bar{s}_\theta(t)$. That is to say, **at inference, we normalise the score estimate with the empirical average absolute pixel value at t of previous score estimates**. The aim of this is to further reduce the variation in the reparameterisation near $t=0$.

$\bar{s}_\theta(t)$ can be found using offline generations at high NFEs. We use linear interpolation to accommodate continuous t . Our approach can be directly plugged into DEIS, so we refer to it as DEIS-SN.

³Note that we focus only on the time-based version of DEIS, tAB.

⁴Note that we simplify notation compared to [25] by restricting ourselves to the case of isotropic noise.

⁵This is corroborated in Fig. 4a of [25]

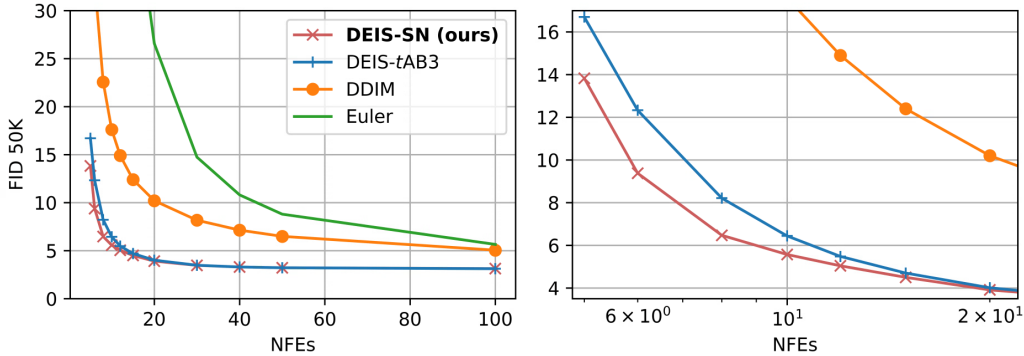


Figure 3: Left: FID 50K for CIFAR-10 against NFEs for different samplers on the same trained model. Right: zoomed in view of the left figure. **DEIS-SN consistently outperforms DEIS at low NFEs.**

We note that gDDIM [26] is another extension to DEIS, however this approach is specifically applicable to data distributions that are well modelled by a single Gaussian (such as the velocity of Critically-Damped Langevin Diffusion [3]), which is not the case for image datasets like CIFAR.

5 Experimental Results

We train the UNet architecture from [15] on CIFAR-10 [10] using the linear β schedule [4] on noise prediction.⁶ We compare our approach to Euler integration of Eq. (4), DDIM [21] and DEIS-*t*AB3 (polynomial order $r=3$) [25]. DEIS-SN is identical to DEIS-*t*AB3 other than the choice of $K_t = 1/\bar{s}_\theta(t)$ over $K_t = \sigma_t$. The average absolute score estimate $\bar{s}_\theta(t)$ is measured offline on a batch of 256 generations. For Euler and DDIM we use trailing linear time steps [11], whilst for DEIS we use trailing quadratic time $i \in \{0, \dots, N\}$, $t_i = (i/N)^2$. For full experimental details see Appendix A. A similar protocol was followed for LSUN-Church (64×64) experiments.

Fig. 3 shows for CIFAR-10, that at low NFEs, DEIS-SN provides a consistent FID improvement over vanilla DEIS. For higher NFEs, when the width of the intervals $[t_{i-1}, t_i]$, and thus the integration error, is reduced, the benefit of DEIS-SN gradually disappears and DEIS-SN performs almost identically to vanilla DEIS. Both DDIM and Euler significantly underperform both DEIS approaches. Experimental results for LSUN-Church are shown in Appendix E.

Fig. 1 shows visual comparisons of vanilla DEIS and DEIS-SN at 5 NFEs.⁷ We see that DEIS-SN can better generate details (such as vehicle wheels). We note that generally generations are visually similar on a high level. This is because the difference between vanilla DEIS and DEIS-SN only occurs for t near 0 (Fig. 2), i.e. the end of the generation/reverse process.

6 Conclusion

In this work we propose to extend the Diffusion Exponential Integrator Sampler (DEIS) with empirical score normalisation (DEIS-SN). Through our novel score-reparameterisation, we aim to further reduce integration error towards the end of the generation process by normalising the score estimate with the empirical average absolute value of previous score estimates. We validate our approach empirically on CIFAR-10 and LSUN-Church, showing that DEIS-SN is able to consistently outperform vanilla DEIS for low NFE generations in terms of FID 50k. We also show visual examples of DEIS-SN’s superiority.

In the future it would be interesting to extend this work to cover non-isotropic cases, where the score reparameterisation K_t is performed by a matrix, possibly in a transformed space such as the frequency domain [1, 5], to see if additional performance gains are to be had. Another possibility would be to parameterise K_t and directly optimise it for better image quality at low NFEs.

⁶Note this is smaller than the architecture used in [22, 25] so the baseline high NFE FIDs are slightly worse.

⁷We select examples with clear visual differences, as many generations are visually indistinguishable. (Nevertheless, the FID 50K results indicate there is a difference in generation quality on aggregate.)

References

- [1] Ayan Das, Stathi Fotiadis, Anil Batra, Farhang Nabiei, FengTing Liao, Sattar Vakili, Da shan Shiu, and Alberto Bernacchia. Image generation with shortest path diffusion. In *International Conference on Machine Learning*, 2023.
- [2] Prafulla Dhariwal and Alexander Nichol. Diffusion models beat gans on image synthesis. *Advances in neural information processing systems*, 34:8780–8794, 2021.
- [3] Tim Dockhorn, Arash Vahdat, and Karsten Kreis. Score-based generative modeling with critically-damped langevin diffusion. In *International Conference on Learning Representations (ICLR)*, 2022.
- [4] Jonathan Ho, Ajay Jain, and Pieter Abbeel. Denoising diffusion probabilistic models. In H. Larochelle, M. Ranzato, R. Hadsell, M.F. Balcan, and H. Lin, editors, *Advances in Neural Information Processing Systems*, volume 33, pages 6840–6851. Curran Associates, Inc., 2020.
- [5] Emiel Hoogeboom and Tim Salimans. Blurring diffusion models. In *The Eleventh International Conference on Learning Representations*, 2023.
- [6] Emiel Hoogeboom, Victor Garcia Satorras, Clément Vignac, and Max Welling. Equivariant diffusion for molecule generation in 3d. In *International conference on machine learning*, pages 8867–8887. PMLR, 2022.
- [7] Tero Karras, Miika Aittala, Timo Aila, and Samuli Laine. Elucidating the design space of diffusion-based generative models. In S. Koyejo, S. Mohamed, A. Agarwal, D. Belgrave, K. Cho, and A. Oh, editors, *Advances in Neural Information Processing Systems*, volume 35, pages 26565–26577. Curran Associates, Inc., 2022.
- [8] Tero Karras, Samuli Laine, Miika Aittala, Janne Hellsten, Jaakko Lehtinen, and Timo Aila. Analyzing and improving the image quality of StyleGAN. In *Proc. CVPR*, 2020.
- [9] Diederik Kingma, Tim Salimans, Ben Poole, and Jonathan Ho. Variational diffusion models. *Advances in neural information processing systems*, 2021.
- [10] Alex Krizhevsky, Geoffrey Hinton, et al. Learning multiple layers of features from tiny images. 2009.
- [11] Shanchuan Lin, Bingchen Liu, Jiashi Li, and Xiao Yang. Common diffusion noise schedules and sample steps are flawed. *ArXiv*, abs/2305.08891, 2023.
- [12] Haohe Liu, Zehua Chen, Yi Yuan, Xinhao Mei, Xubo Liu, Danilo Mandic, Wenwu Wang, and Mark D Plumbley. Audioldm: Text-to-audio generation with latent diffusion models. *arXiv preprint arXiv:2301.12503*, 2023.
- [13] Cheng Lu, Yuhao Zhou, Fan Bao, Jianfei Chen, Chongxuan LI, and Jun Zhu. Dpm-solver: A fast ode solver for diffusion probabilistic model sampling in around 10 steps. In S. Koyejo, S. Mohamed, A. Agarwal, D. Belgrave, K. Cho, and A. Oh, editors, *Advances in Neural Information Processing Systems*, volume 35, pages 5775–5787. Curran Associates, Inc., 2022.
- [14] Cheng Lu, Yuhao Zhou, Fan Bao, Jianfei Chen, Chongxuan Li, and Jun Zhu. DPM-solver++: Fast solver for guided sampling of diffusion probabilistic models, 2023.
- [15] Alexander Quinn Nichol and Prafulla Dhariwal. Improved denoising diffusion probabilistic models. In Marina Meila and Tong Zhang, editors, *Proceedings of the 38th International Conference on Machine Learning*, volume 139 of *Proceedings of Machine Learning Research*, pages 8162–8171. PMLR, 18–24 Jul 2021.
- [16] Ben Poole, Ajay Jain, Jonathan T Barron, and Ben Mildenhall. Dreamfusion: Text-to-3d using 2d diffusion. *arXiv preprint arXiv:2209.14988*, 2022.
- [17] Robin Rombach, Andreas Blattmann, Dominik Lorenz, Patrick Esser, and Björn Ommer. High-resolution image synthesis with latent diffusion models. In *Proceedings of the IEEE/CVF conference on computer vision and pattern recognition*, pages 10684–10695, 2022.
- [18] Tim Salimans and Jonathan Ho. Progressive distillation for fast sampling of diffusion models. In *International Conference on Learning Representations*, 2022.
- [19] Tim Salimans, Andrej Karpathy, Xi Chen, and Diederik P. Kingma. Pixelcnn++: A pixelcnn implementation with discretized logistic mixture likelihood and other modifications. In *ICLR*, 2017.
- [20] Jascha Sohl-Dickstein, Eric Weiss, Niru Maheswaranathan, and Surya Ganguli. Deep unsupervised learning using nonequilibrium thermodynamics. In Francis Bach and David Blei, editors, *Proceedings of the 32nd International Conference on Machine Learning*, volume 37 of *Proceedings of Machine Learning Research*, pages 2256–2265, Lille, France, 07–09 Jul 2015. PMLR.
- [21] Jiaming Song, Chenlin Meng, and Stefano Ermon. Denoising diffusion implicit models. In *International Conference on Learning Representations*, 2021.
- [22] Yang Song, Jascha Sohl-Dickstein, Diederik P Kingma, Abhishek Kumar, Stefano Ermon, and Ben Poole. Score-based generative modeling through stochastic differential equations. In *International Conference on Learning Representations*, 2021.

- [23] Patrick von Platen, Suraj Patil, Anton Lozhkov, Pedro Cuenca, Nathan Lambert, Kashif Rasul, Mishig Davaadorj, and Thomas Wolf. Diffusers: State-of-the-art diffusion models. <https://github.com/huggingface/diffusers>, 2022.
- [24] Daniel Watson, William Chan, Jonathan Ho, and Mohammad Norouzi. Learning fast samplers for diffusion models by differentiating through sample quality. In *International Conference on Learning Representations*, 2021.
- [25] Qinsheng Zhang and Yongxin Chen. Fast sampling of diffusion models with exponential integrator. In *The Eleventh International Conference on Learning Representations*, 2023.
- [26] Qinsheng Zhang, Molei Tao, and Yongxin Chen. gDDIM: Generalized denoising diffusion implicit models. In *The Eleventh International Conference on Learning Representations*, 2023.
- [27] Hongkai Zheng, Weili Nie, Arash Vahdat, Kamyar Azizzadenesheli, and Anima Anandkumar. Fast sampling of diffusion models via operator learning. In *International Conference on Machine Learning*, 2023.

A Additional Experimental Details

In order to perform sampling with our proposed method, and for comparison purposes, we trained a model to approximate the true score $\nabla_{\mathbf{x}_t} \log p(\mathbf{x}_t)$ with a standard architecture and training procedure. We purposefully use a model with relatively small capacity to segregate the effects of sampling procedure and better score estimation [7, 22]. We train our score estimator in a discrete DDPM Ho et al. [4] setup with time-discretization granularity $N = 1000$, $i \in \{0, \dots, N\}$, $t_i = i/N$, which is considered to be a standard in diffusion literature. As suggested by Ho et al. [4], we train the score estimator with the “simple loss” which is proven to be better at generation quality, as opposed to the true variational bound [9]. Again, as per Ho et al. [4], we do not directly estimate the score s_θ , but instead estimate the “noise-predictor” ϵ_θ . Concretely, We optimize the following objective,

$$\mathbb{E}_{\mathbf{x}_0 \sim p(\mathbf{x}_0), \mathbf{x}_t \sim p(\mathbf{x}_t | \mathbf{x}_0), i \sim \mathcal{U}\{1, N\}, \epsilon \sim \mathcal{N}(0, I)} [\|\epsilon_\theta(\mathbf{x}_{t_i}, t_i) - \epsilon\|_2^2], \quad (6)$$

where $p(\mathbf{x}_0)$ is the data distribution realized using our dataset, the forward noising conditional $p(\mathbf{x}_t | \mathbf{x}_0)$ is from Eq. (1) and t_i are timesteps. We use the standard “positional embeddings” for incorporating t_i into the noise-estimator neural network. The (a_t, σ_t) in Eq. (1) are chosen to be the standard “linear schedule” and *variance-preserving* formulation [22], *i.e.*

$$a_t^2 = \prod_{t'=1}^t (1 - \beta_{t'}), \text{ and } \sigma_t = \sqrt{1 - a_t^2} \quad (7)$$

where $\beta_t = \beta_{min} + (\beta_{max} - \beta_{min}) \cdot t$ with $\beta_{min} = 10^{-4}$ and $\beta_{max} = 2 \times 10^{-2}$. To obtain continuous time a_t we employ simple linear interpolation as in [25]. We use the AdamW optimizer with learning rate 10^{-4} and no gradient clipping. We also use the standard process of using *Exponential Moving Average (EMA)* while training the network ϵ_θ using Eq. (6). We used a minibatch size of 128 on each of 4 GPUs, making the effective batch size 512. We trained for 2000 epochs on both CIFAR-10 [10] and LSUN-Church constituting 196k iterations and simply chose the final checkpoint. For faster training, we used mixed-precision training, which did not degrade any performance as per our experiments. The architecture of the U-Net used as ϵ_θ is taken exactly to be the standard architecture proposed in iDDPM [15], with a dropout rate of 0.3. All our experiments are implemented using the `diffusers` library [23].⁸

When generating samples for evaluation, we set the random seed to be the same value across all experiments. This allows a better comparison between different ODE sampling methods as different samplers will still follow similar trajectories (see Fig. 1).

B Mathematical Simplifications

We note that a number of simplifications/analytic results can be leveraged for DEIS, when applied specifically to the variance preserving process [4, 25],

$$\sigma_t^2 = 1 - a_t^2, \quad g_t^2 = -2f_t, \quad \Psi(t, s) = a_t/a_s. \quad (8)$$

C DEIS-SN Implementation Details

We follow Zhang and Chen [25]’s DEIS implementation⁹ closely for the most part. One minor difference is that we set $t_0 = 0$ rather than a small value such as 10^{-4} . We find that for the samplers that we use this does not lead to any discontinuities/divide-by-zero errors, since no function is actually evaluated at $t = 0$ (Eq. (5) uses a one-sided Riemann sum for numerical integration).

We find empirically that performance is improved by truncating $\bar{s}_\theta(t)$ slightly, close to $t = 0$. This is possibly due to numerical instability from its rapid increase as $\sigma_t \rightarrow 0$. We simply set $\bar{s}_\theta(t) = \bar{s}_\theta(0.005)$ for $t < 0.005$. We calculate $\bar{s}_\theta(t)$ by measuring the average absolute pixel values of $s_\theta(\mathbf{x}_t, t)$ at each time step using DEIS-tAB3 with 1000 NFEs (1000 uniform time steps) over

⁸<https://github.com/huggingface/diffusers/tree/main>

⁹https://github.com/qsh-zh/deis/tree/main/th_deis

a batch of 256 generations. This is done using a different random seed to the generations used for evaluation. We then use linear interpolation to obtain values over continuous time.

D More generation results

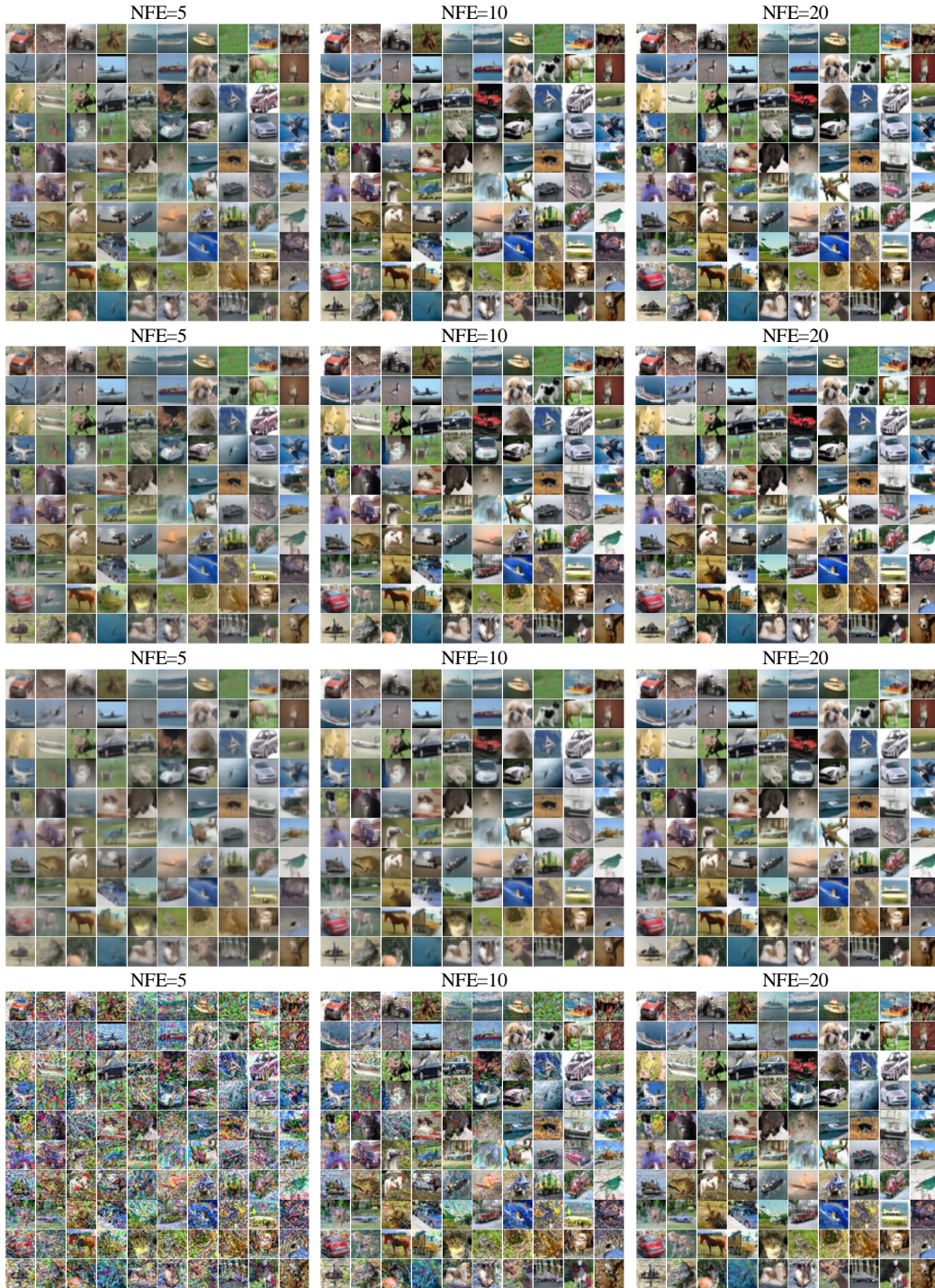


Figure 4: Visual comparison of unconditional samples for CIFAR10 generated (with same seed) at relatively low NFE for (top to bottom) **DEIS-SN (Ours)**, DEIS, DDIM & Euler sampler.

E Results on LSUN-Church

We follow exactly same protocol except the UNet architecture, which in this case is adapted from [2]. The UNet in question has an attention resolution of only 16 (unlike 16,8 in CIFAR-10 model) and 2 ResNet blocks (unlike 3 in CIFAR-10 model). We also use a dropout of 0.1 while training out LSUN-Church model. Below, in Fig. 5, we present the FID-vs-NFE curves similar to Fig. 1 in the main paper.

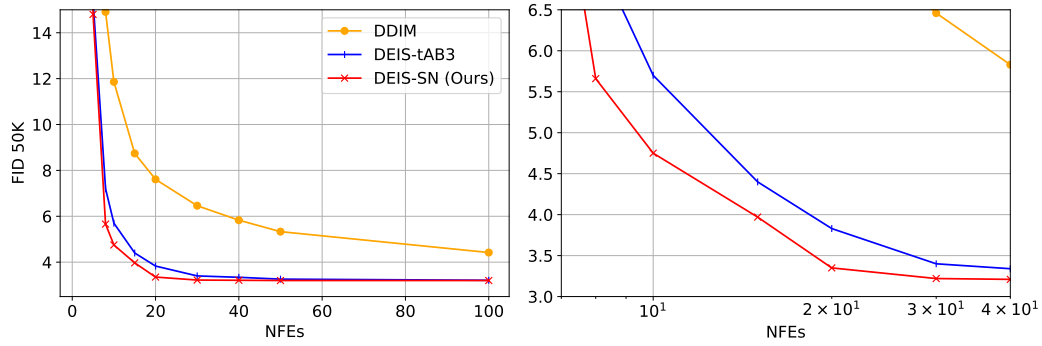


Figure 5: Left: FID 50K for LSUN-Church against NFEs for different samplers on the same trained model. Right: zoomed in view of the left figure. **DEIS-SN consistently outperforms DEIS at low NFE regime.**